Eur Biophys J (1990) 18:203–219

European Biophysics Journal

Bending undulations and elasticity of the erythrocyte membrane: effects of cell shape and membrane organization

K. Zeman, H. Engelhard, and E. Sackmann

Physik Department, Technische Universität München, D-8046 Garching bei München, Federal Republic of Germany

Received September 5, 1989/Accepted in revised form January 2, 1990

Abstract. The undulatory excitations (flickering) of human and camel erythrocytes were evaluated by employing the previously used flicker spectroscopy and by local measurements of the autocorrelation function $K(t)$ of the cell thickness fluctuations using a dynamic image processing technique. By fitting theoretical and experimental flicker spectra relative values of the bending elastic modulus K_c of the membrane and of the cytoplasmic viscosity η were obtained. The effects of shape changes were monitored by simultaneous measurement of the average light intensity I_0 passing the cells and by phase contrast microscopic observation of the cells. Evaluation of the cellular excitations in terms of the quasi-spherical model yielded values of K_c/R_0^3 and $\eta \cdot R_0$ (R_0 = equivalent sphere radius) and allowed us to account (*1*) for volume changes, (*2*) for effects of surface tension and spontaneous curvature and (*3*) for the non-exponential decay of $K(t)$. From the long time decay of $K(t)$ we obtained an upper limit of the bending elastic modulus of normal cells of $K_c = 2-3 \cdot 10^{-19}$ Nm which is an order of magnitude larger than the value found by reflection interference contrast microscopy (RICT, $K_c = 3.4 \cdot 10^{-20}$ Nm, Zilker et al. 1987) but considerably lower than expected for a bilayer containing 50% cholesterol ($K_c = 5 \cdot 10^{-19}$ Nm, Duwe et al. 1989). The major part of the paper deals with long time measurements (order of hours) of variations of the apparent K_c and η values of single cells (and their reversibility) caused (*1*) by osmotic volume changes, (*2*) by discocyte-stomatocyte transitions induced by albumin and triflouperazine, (*3*) by discocyte-echinocyte transitions induced by expansion of the lipid/protein bilayer (by incubation with lipid vesicles) and by ATP-depletion in physiological NaCl solution, (*4*), by coupling or decoupling of bilayer and cytoskeleton using wheat germ agglutinin or erythrocytes with elliptocytosis and (*5*) by cross-linking the cytoskeleton using diamide. These experiments showed: (*1*) K_c and η are minimal at physiological osmolarity and temperature and well controlled over a large range of these parameters. (*2*) Echinocyte formation does not markedly alter the apparent membrane bending stiffness. (*3*) During swelling the cell may undergo a transient discocyte-stomatocyte transition. (*4*) Strong increases of the apparent K_c and η after cup-formation or strong swelling and deflation are due to the effect of shear elasticity and surface tension. Our major conclusions are: (*1*) The erythrocyte membrane exhibits a shear free deformation regime which requires ATP for its maintenance. (*2*) Shape transitions may be caused by relative area changes either of the two monolayers of the lipid/protein bilayer (corresponding to the bilayer coupling hypothesis) or of the bilayer and the cytoskeleton where the latter mechanism appears to be more frequent. (*3*) The low bending stiffness and the shear free deformation regime are explained in terms of a slight excess area of the lipid bilayer leading to a pre-undulated surface profile. Freeze fracture electron microscopy studies provide direct evidence for a pre-undulated bilayer with an undulation wavelength of approximately 100 nm.

Key words: Membrane elasticity – Erythrocyte membrane – Flickering – Membrane bending undulations

Introduction

The red blood cell is an elastic shell with remarkable properties. Its lateral compressibility modulus is comparable to that of technical materials (such as polyethylene) whereas its shear and bending elastic constants are orders of magnitude smaller (Evans and Needham 1986; Duwe et al. 1989). The low resistance towards bending and shearing together with the non-spherical shape allows the cells to squeeze through very narrow blood capillaries. The high lateral stiffness, however, is essential to prevent strain induced leakage of ions through the membrane. These remarkable elastic properties of the erythrocyte membrane are achieved by the combination of two states of matter: (*1*) the smectic liquid crystaline lipid/protein bilayer and (*2*) the quasi-two dimensional macromolecular spectrin-actin network which is loosely cou-

Offprint requests to: E. Sackmann

pled to the bilayer. Since the bending elastic constant K_c is of the order of $k_B T$ the erythrocyte membrane exhibits pronounced thermally excited undulations, the so-called flickering (Brochard and Lennon 1975; Fricke et al. 1986). Therefore the erythrocyte can also be considered as an interesting model for a (closed) random surface (Leibler et al. 1987).

The primary reason for the growing interest in the viscoelastic properties of erythrocytes is, however, based on the hope that measurements of the elastic and viscous parameters will yield valuable insights into the membrane structure and – more importantly – allow us to detect subtle changes of the membrane structure caused by diseases or drugs. It is for these reasons that a whole range of techniques enabling the measurement of the various viscoelastic parameters of vesicles and cells have been developed. These include the various micropipette techniques (Evans and Skalak 1980; Hochmut et al. 1979; Waugh 1987), the electric field deformation technique (Engelhardt and Sackmann 1988), the cell poking technique (Petersen et al. 1982), the Ektocytometer technique (Bessis and Mohandas 1975) and flicker spectroscopy (Fricke et al. 1986; Zilker et al. 1987).

In the present work flicker spectroscopy has been applied in order to study the bending undulations of erythrocytes as a function of physically and chemically induced changes of the membrane structure and cell shape. Two strategies were followed: *(1)* The simultaneous measurement of the bending elastic modulus K_c, the cytoplasmatic viscosity η and the average transmitted light intensity I_0 in order to distinguish carefully between effects of shape changes and true modifications of the membrane structure and dynamics, *(2)* the continuous measurements (over hours) of the temporal variations of these parameters induced by various physical and biochemical stresses. Two techniques were applied: Firstly, frequency spectrum analysis of the intensity fluctuations of the light passing the cell and secondly, measurements of the autocorrelation function at local areas of the cell by dynamic image processing. Furthermore the flicker spectra were analyzed in terms of a quasi-spherical model (Peterson 1985; Schneider et al. 1984) instead of the classical Brochard and Lennon theory (1975). The former approach is better suited to account for the influence of shape changes, chemically induced bending moments and surface tension effects. It is, however, only valid for moderatly swollen cells.

Experimental techniques

Buffers

Three types of buffer were used:

1) Buffer with albumin (cf. Fricke et al. 1986), consisting of 123 m*M* NaCl (for adjustment of osmolarity), 25 m*M* glucose, 11 m*M* Na_3-citrate (a Ca^{++}-complex former which acts as anticoagulant), 0.1 m*M* adenine, 0.1 m*M* inosine. The pH is adjusted to pH 7.4 using 300 m*M* citric acid. In addition the buffer contained 1 vol% of a vitamin-solution (No. K2731 from Seromed, Biochrom KG, Berlin, FRG) and 1 vol% of an antibiotic-solution (penicillin/streptomycin 100 I.E./ml, No. A2213 from Seromed, Biochrom KG, Berlin, FRG). 2.5 mg/ml albumin (bovine serum albumin, Fraction V, Serva) stabilizes the shape of the erythrocytes inside the measuring chamber. Without this protein in the buffer the cells transform immediately to echinocytes.

2) Buffer with fetal calf serum and albumin, consisting of 103 m*M* NaCl, 25 m*M* glucose, 11 m*M* Na_3-citrate, 5 m*M* KCl, 3 m*M* $CaCl_2$, 2 m*M* $MgCl_2$, 0.1 m*M* adenine, 0.1 m*M* inosine, 1 vol% vitamin- and 1 vol% antibiotic-solution. To the buffer was added 1.5 mg/ml albumin and 3 vol% fetal calf serum (purchased from Boehringer Mannheim, FRG). The pH was adjusted to pH 7.4 as above. Serum increases the lifetime of erythrocytes in vitro for several reasons. It contains lipids which prevent loss of this membrane constituent by the cell (Shohet and Nathan 1970) and it probably closes K^+-channels and thereby decreases ion exchange between cytoplasm and buffer (Dall-Asta et al. 1986).

3) Buffer with autologuous serum, consisting of 108 m*M* NaCl, 25 m*M* glucose, 11 m*M* Na_3-citrate, 5 m*M* KCl, 3 m*M* $CaCl_2$, 2 m*M* $MgCl_2$, 0.1 m*M* adenine, 0.1 m*M* inosine, 1 vol% vitamin- and 1 vol% antibiotic-solution. 2 vol% autologuous serum (serum and erythrocytes from the same donor) was added; this was prepared as follows: 10 ml blood are taken from the arm vein without anticoagulant, stirred with a glass-rod until coagulation and centrifuged (at 2000 *g*, 5 min). The pH of the buffer was adjusted to pH 7.4 as above.

Immediately after being transferred into one of the first two types of buffer, the cells showed an initial cup-formation caused by the albumin. They were therefore pre-incubated for two hours until they regained their original biconcave shape and the measurement could be started. In the fetal calf serum-containing buffer the lifetime of the cells was prolonged. No shape changes were observed within 5 h, in contrast to the cells in buffer which contain only albumin (cf. Fig. 7 b). A disadvantage of the serum however is that it is more difficult to fix the cells to the glass plates using polylysine. In the buffer with autologuous serum the cells did not exhibit the initial cup formation but their lifetime was only 2–3 h before spherocyte formation.

Cell preparation

For most of the experiments blood (2 µl) was taken from the finger tip, diluted in 1 ml buffer and preincubated for two hours. Larger quantities were drawn from the arm vein with Na_3-citrate as anticoagulant. The erythrocytes were harvested by centrifugation of the blood at 2000 *g* for 5 min and removal of the supernatant (plasma and white blood cells). In some cases the cells were further washed three times by centrifugation and dilution with the wash solution.

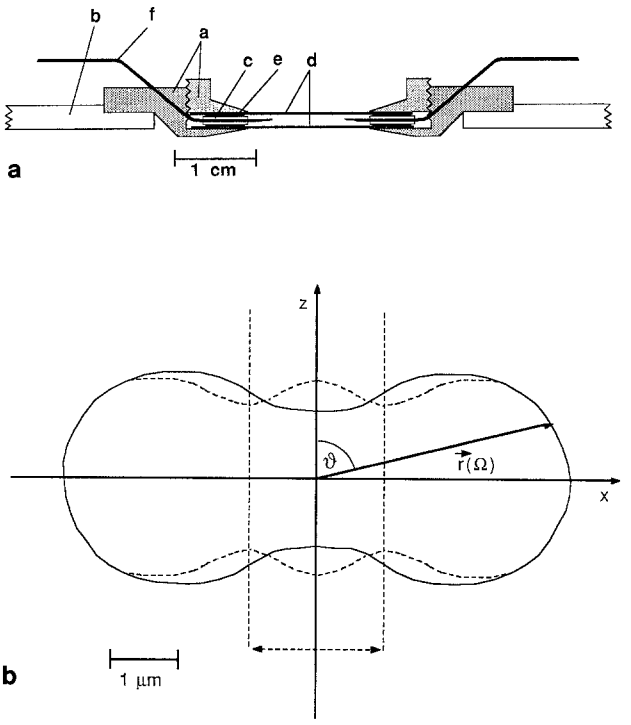

Fig. 1. **a** Measuring chamber used for both measuring procedures, the frequency spectrum analysis of the intensity fluctuations using a Zeiss Photomicroscope and the correlation function analysis by image processing using a Zeiss Axiomat microscope. In the former case the cells are fixed to the bottom and in the latter to the top window of the chamber. The parts are: *a)* brass chamber with screwable cover, *b)* plexiglass holder, *c)* gilded brass ring-disk with two bore holes for the tubes, *d)* cover glasses (20 × 20 mm), *e)* packing rings of Parafilm and *f)* tubes with a diameter of 0.6 mm for rinsing the chamber during measurement. **b** Schematic view of erythrocyte in resting (—) and excited (- - -) state and definition of the rotational symmetry axis z, symmetry plane xy, polar angle ϑ, and radius vector $\boldsymbol{r}(\Omega)$ from origin to cell surface. The dash-point lines mark the area of observation in frequency spectrum analysis

Measuring chamber

For both types of measurement the same measuring chamber, shown in Fig. 1, was used. The cover of the chamber could be screwed off in order to allow exchange of the windows and to facilitate cleaning. In order to load the erythrocytes into the chamber it was first filled with buffer which was pumped through the tubes using a peristaltic pump until removal of all air bubbles. Then a few microlitres of the cell suspension were pumped in. After waiting for 10–20 min enough cells had sedimented and were fixed to the bottom glass plate which had been pretreated with polylysine. The residual cells were then pumped out. In order to cover the windows with polylysine (poly-D, L-lysine hydrobromide, MW: 3000 g, purchased from Sigma) they were washed with Millipore water and then with ethanol. After drying they were dipped for a few seconds in a 5 mM solution of polylysine in water (cf. Fricke and Sackmann 1984).

Methods of evaluation of thickness fluctuations

Two techniques were applied: (*1*) frequency spectrum analysis of the intensity fluctuations of the light passing a small area located in the center of the cell, (*2*) analysis of the temporal intensity correlation function of the light passing local areas of the cell by dynamic image processing.

1. Frequency spectrum analysis. This technique has been described previously (Fricke et al. 1986). A Zeiss Photomicroscope III was used. Illumination occurred with an incandescent lamp (12 V, 60 W, Zeiss). Infrared light was filtered out using an optical filter (from Schott KG, FRG) with a cut-off at 650 nm. The cells were observed with a phase contrast oil immersion objective (× 100/1.25, 0.17, Ph 3, Planachromat from Zeiss, FRG). Images of the cell were taken with the built in camera of the microscope or focussed onto a photomultiplier (RCA, PF 1006) or a photodiode attached to the microscope. The output of these detectors was fed to a Hewlett Packard Frequency Analyser (HP 3582A).

As noted previously it is essential to measure only in the center of the cells in order to minimize intensity fluctuations caused by their lateral Brownian motions. For this purpose an aperture of 0.5 mm diameter was positioned in front of the photodetector. An area with a diameter of 2 μm was observed. The frequency analyser yields the frequency spectrum $F(\omega)$ of the photodetector output voltage. Since the latter is proportional to the intensity I, $F(\omega)$ is proportional to the square root of the power spectrum $P(\omega, q)$ of the intensity fluctuation (cf. (1) to (3) according to Brochard and Lennon 1975). To obtain relative values of the bending stiffness K_c and the cytoplasmatic viscosity η the square root of the integrated theoretical power spectrum $P(\omega)$ was fitted to the measured frequency spectrum $F(\omega)$ as described in the appendix. The amplitudes of the frequency spectrum $F(\omega)$ are proportional to the average light intensity I_0. To obtain intensity corrected values for K_c and η the measured frequency spectra $F(\omega)$ were normalized by dividing by I_0. Typical, normalized frequency spectra are shown in Fig. 2 together with the fitted curves for different osmolarities of the buffer. As can be clearly seen the spectra change in a characteristic way with the osmolarity and the agreement between experimental and fitted curves is excellent.

2. Correlation function analysis. For the second technique an inverted Zeiss Axiomat microscope equipped with a home made fast image processing system was used. The latter has been described previously (Engelhardt and Sackmann 1988; Zilker et al. 1987). Images of the cells were recorded at a rate of 50 half images per second and the intensity values of several measured points r were stored in the memory of the image processor. Then the autocorrelation function of the intensity fluctuations $K(t) = \langle \delta I(r, t)\, \delta I(r, 0) \rangle$ was determined for the different positions r on the cell.

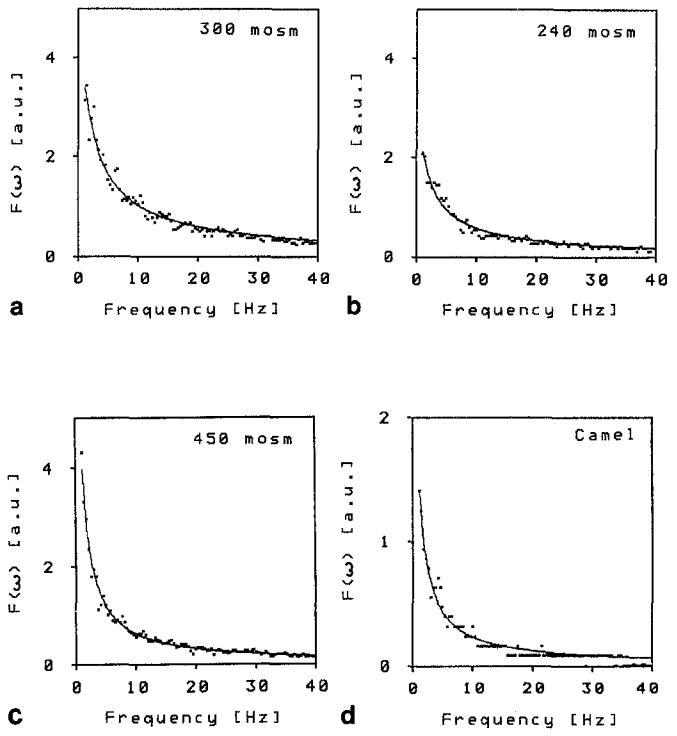

Fig. 2a–c. Variation of the frequency spectrum $F(\omega)$ of the photomultiplier output (which is proportional to the intensity fluctuations of the light passing the cell) with osmolarity. Dots: data from frequency analyzer; drawn line: spectrum fitted by (16). Note that during the transition from 300 to 240 mosm the amplitude $F(\omega)$ decreases at all frequencies about equally whereas at 450 mosm the amplitudes is strongly suppressed at high frequencies but amplified when ω goes to 0. Note: a.u. means arbitrary units. **d** Frequency spectrum of a camel erythrocyte at 300 mosm

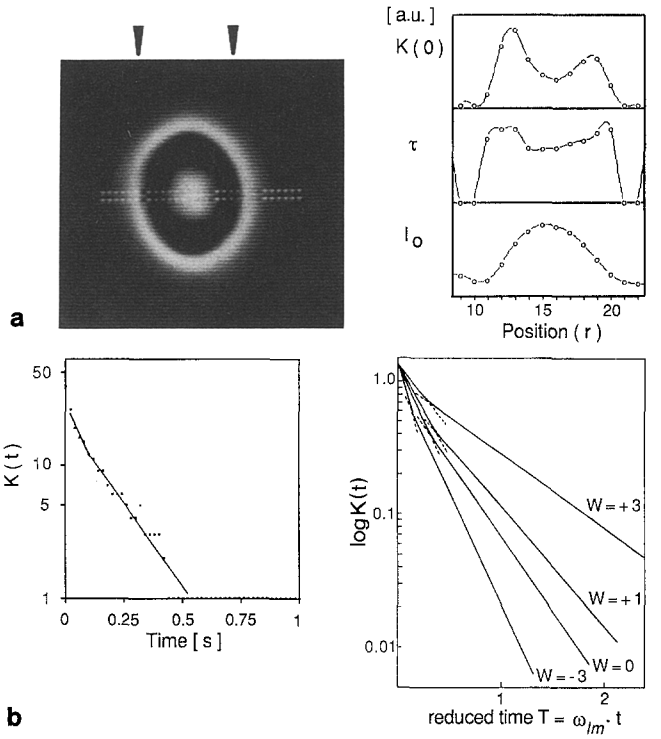

Fig. 3. a Evaluation of the intensity correlation function of the light passing the cell using fast image processing. *Left:* Red blood cell with two rows of white measurement points ($2 \cdot 30$ points), the arrows mark the limits of the right figure. *Right:* Plot of the maximum amplitude $K(0)$ of the intensity autocorrelation function $K(t, \omega)$ (top row), its correlation time τ and the average intensity I_0 of the light passing the cell as a function of the position r. The plotted values are always averaged values of two neighboring measurement points. **b** *Left:* Typical autocorrelation functions obtained from one point located in the center of the cell (measuring time 200 s). Note the non-exponential behavior in the log $K(t)$-versus-t-plot. The slow and the fast correlation times are $\tau = 0.09$ s and $\tau = 0.16$ s, respectively. *Right:* The theoretical correlation function $K(t)$ of the thickness fluctuations is calculated with (9) and (10) for four values of the sum $W = -\tilde{\gamma} - 4w + 2w^2$; $W = -3, 0, +1, +3$. All curves are normalized at $K(t=0)$. Note the pronounced non-exponential decay in particular for $w \approx 0$

Figure 3 shows a typical result. In Fig. 3b the maximum amplitude $K(0)$ and the correlation time τ of the autocorrelation function $K(t, q)$ (5) and the average intensity I_0 are plotted for different positions along a section through the cell center (cf. Fig. 3a). The intensity I_0 varies strongly as expected. Since the amplitudes $K(t)$ are proportional to I_0^2 large errors are caused by diffraction effects. These are particularly large in the outer regions of the cell where the thickness varies widely. It is therefore not possible to obtain reliable values of K_c according to (5) in this region. The viscoelastic parameters can thus only been evaluated in the central area of cells.

In Fig. 3b a measured correlation function $K(t)$ is compared with a theoretical curve calculated using the quasi-spherical model as shown in the next section. Both curves exhibit clearly non-exponential behavior. It is important to realize that the two methods are complementary. The frequency analysis of the undulations is more sensitive with respect to the long time behavior and is thus better suited to study the long wavelength excitations. The second method is more appropriate to evaluate the short time behavior. A further advantage of the second method is that it may also be used to determine the spatial-temporal correlation function of the thickness fluctuations.

Theoretical background of flicker spectroscopy

The present analysis of the membrane excitations in terms of cellular thickness fluctuations is fast and experimentally easy to realize. However, it suffers from the fact that it averages over all excitation modes q in contrast to the recently developed reflection interference contrast technique (RICT), which shows, that the flicker spectrum is mainly determined by the lowest order modes (Zilker et al. 1987). It is thus difficult to distinguish between effects caused by changes in the cell shape and the bending rigidity because the former affect the lowest order modes most strongly. In the present work this problem was partially overcome by simultaneous measurement of the average intensity of the light passing the cell, whereby changes of the cell shape were detected.

Previously, (Fricke et al. 1986) we interpreted the flicker spectra in terms of the approach of Brochard and Lennon (1975) where the cell is treated as two parallel planar bilayers. This is a reasonably good approximation

for excitation wavelengths small compared to the cell diameter. According to Zilker et al. (1987) this holds for wavelengths ≤ 1 μm. Since the flicker spectra are dominated by the lowest order modes the above model breaks down. To account for the coupling of the opposing membranes of the cell Brochard and Lennon introduced the peristaltic mode concept which would, however, only be a reasonably good approximation if the cell diameter was large compared to the inter-membrane distance, which is not the case.

In the present work we take another approach which is better adapted to the topology of the red blood cell. We treat the cell as a quasi-spherical shell and interpret the flicker spectra in terms of the theory of shape fluctuations of quasi-spherical vesicles (Schneider et al. 1984; Peterson 1985; Millner and Safran 1987). This model allows us to account for the surface tension and spontaneous curvature effects in a quantitative way. In both approaches (the independent planar membrane and the quasi-spherical model) each excitation mode of the wave vector q contributes a Lorentzian line of the form:

$$P(q, \omega) = \frac{P_0}{(\omega_q^2 + \omega^2)} \tag{1}$$

In the following the total flicker spectrum obtained by integration or summation over all wave vectors q is considered separately.

1. The Brochard and Lennon approach

By assuming that the cell consists of two independently excited membranes one has

$$P_0 = \frac{S k_B T}{\pi \eta q} \tag{2}$$

$$\omega_q = \frac{K_c q^3}{2\eta} \tag{3}$$

where S is the area of the cell, K_c the bending elastic modulus, η the viscosity of the cytoplasm and q the absolute value of the wave vector in the plane of the membrane. The total power spectrum $P(\omega)$ is obtained by integration of (1) with (2) and (3) over all wave vectors q between a lower limit $q_{\min}$ and an upper limit $q_{\max}$ (cf. Appendix).

$$P(\omega) = \int_{q_{\min}}^{q_{\max}} P(q, \omega)\, 2\pi q \, \mathrm{d}q \tag{4}$$

$q_{\min}$ is determined by the cell diameter (≈ 7.5 μm) and is $q_{\min} \approx 1\ \mu\mathrm{m}^{-1}$. $q_{\max}$ is determined by the diameter of the observed area of the cell (≈ 2 μm) and is $q_{\max} \approx 3\ \mu\mathrm{m}^{-1}$. Fortunately, $P(\omega)$ depends only weakly on the integration limits. In the order to determine K_c and η the square root of $P(\omega)$ is fitted to the experimental frequency spectra $F(\omega)$ as described in the Appendix. The Fourier transformation of (1) with (2) and (3) yields the autocorrelation function $K(t, q)$ of the flickering.

$$K(t, q) = \frac{S k_B T}{q^4 K_c} \mathrm{e}^{-\frac{K_c q^3 t}{2\eta}} \tag{5}$$

It is possible to determinate K_c and η from the amplitude $K(0)$ and the correlation time τ of the measured correlation functions.

2. The quasi-spherical approach

Inspection of the erythrocyte shape fluctuations by phase contrast microscopy using the image processing system and the RIC-technique (Zilker et al. 1987) shows that the amplitudes along the equator of the cell are much smaller (≤ 0.1 μm) than in the direction of the rotation symmetry axis (≈ 0.3 μm). This suggests that the excitations of the cell can be approximately described in terms of a restricted set of spherical harmonics with polar axis parallel to the symmetry axis of the cell (cf. Fig. 1 b). Further justification for this approach is provided by Monte Carlo simulations of shape changes of two-dimensional vesicles by Leibler et al. (1987). Following the procedure of Peterson (1985) and Millner and Safran (1987) the fluctuating cell surface is described in terms of a radius (unit) vector $\boldsymbol{r}_0$:

$$\boldsymbol{r}(\vartheta, \varphi, t) = R_0 \left[1 + \sum_{l,m} u_{l,m}(t)\, Y_{l,m}(\vartheta, \varphi) \right] \tag{6}$$

where R_0 is equal to the radius of a sphere with the same volume V_c as the cell: $R_0 = \sqrt[3]{3 V_c / 4\pi}$. In the following R_0 is called the equivalent sphere radius (Millner and Safran 1987). $Y_{l,m}(\vartheta, \varphi)$ are the surface spherical harmonics and $u_{l,m}(t)$ the amplitudes accounting for the displacement of the cell membrane. The mean square value of the amplitudes $u_{l,m}$ are determined by the equipartition theorem according to (cf. Millner and Safran 1987, (10)):

$$\langle |u_{l,m}|^2 \rangle = \frac{k_B T}{K_c} \{(l+2)(l-1)[l(l+1) - 4w + 2w^2 - \tilde{\gamma}]\}^{-1} \tag{7}$$

where $\tilde{\gamma} = \gamma R_0^2 / K_c$ and $w = R_0 H_s$. The Langrange multiplier $\tilde{\gamma}$ accounts for the constraint of finite area and is a measure for the lateral tension which arises for excitation modes requiring an expansion of the cell surface. The parameter w takes into account an intrinsic (average) spontaneous curvature H_s of the cell, which is caused by chemically induced bending moments (Helfrich 1973; Evans 1973). In the above equation the sign convention of Millner and Safran (1987) for γ is used, that is γ is negative, (cf. also Sackmann and Duwe 1990).

The thickness autocorrelation function $K(t)$ in the direction of the cell symmetry axis is now easily obtained from the autocorrelation function of the radius vector $\boldsymbol{r}(\vartheta, \varphi, t)$. By assuming that all modes are excited about a common z-axis one can average over the angle φ and obtains finally

$$\begin{aligned} K(t) &= \langle \delta \mathrm{d}(\vartheta, t)\, \delta \mathrm{d}(\vartheta, 0) \rangle = \langle \delta r(\vartheta, t)\, \delta r(\vartheta, 0) \rangle \cos^2 \vartheta \\ &= 2 R_0^2 \sum_{l,m} (1 + (-1)^{l-m}) \langle u_{l,m}(t)\, u_{l,m}(0) \rangle P_{l,m}^2(\vartheta) \cos^2 \vartheta \end{aligned} \tag{8}$$

where $P_{l,m}(\vartheta)$ are the Legendre polynomials. Owing to the symmetry relation $P_{l,m}(-x) = -1^{(l-m)} P_{l,m}(x)$. It follows

therefore that those excitations for which $(l-m)$ is an odd number do not contribute to the thickness fluctuations since they correspond to a shift of both membranes in the same direction. The correlation function $K(t)$ is now easily obtained by using the results of Peterson (1985) or Millner and Safran (1987: (10) and (12)).

$$K(t) = 4R_0^2 \sum_{l,m} \langle |u_{l,m}|^2 \rangle I_{l,m} \exp(-\omega_{l,m} t) \tag{9}$$

where

$$\omega_{l,m} = \frac{K_c}{\eta R_0^3} \frac{l(l+1) - 4w + 2w^2 - \tilde{\gamma}}{Z(l)} \tag{10a}$$

$$Z(l) = \frac{(2l+1)(2l^2+2l-1)}{(l-1)l(l+1)(l+2)} \tag{10b}$$

and

$$I_{l,m} = \frac{(l+1/2)(l-m)!}{(l+m)!} \int_0^{\vartheta_0} P_{l,m}^2(\cos\vartheta) \cos^2\vartheta \sin\vartheta \, d\vartheta \tag{10c}$$

The integration limit ϑ_0 is determined by the diameter of the area over which the cell is observed. In our case this area corresponds to $\cos\vartheta \approx 1/2$. If the light was only analyzed in the cell center (for instance by image processing) $I_{l,m}$ would be determined by the polynomials with even values of l alone. The frequency power spectrum $P(l, \omega)$ is obtained by Fourier transformation of (9) and is of the form:

$$P(l, \omega) = \sqrt{\frac{32}{\pi}} \frac{k_B T}{\eta R_0} \sum_{l,m} \frac{I_{l,m} W_l}{\omega^2 + \omega_{l,m}^2} \tag{11}$$

where $W_l = (l-1)(l+2) Z(l)$. The dash at the symbol of the sum indicates that it runs only over all even values of $l-m$. $P(l, \omega)$ is equivalent to the Power spectrum $P(\omega, q)$ of the Brochard and Lennon model (1)–(3). However the ill-defined area S is replaced by the measurable equivalent sphere radius R_0. Equations (10) and (11) suggest that one should define normalized values of the viscosity η and the bending stiffness K_c according to:

$$\eta' = \eta R_0 \tag{12a}$$

and

$$K_c' = K_c / R_0^3 \tag{12b}$$

The correlation function $K(t)$ has been calculated for four values of the sum $W = -\tilde{\gamma} - 4w + 2w^2$ (namely for $W = +3; +1; 0; -3$), the corresponding $K(t)$-versus-(t) plots are shown in Fig. 3 b. For 300 mosm the normalized spontaneous curvature $w = R_0 H_s \approx -2$ (Deuling and Helfrich 1976). Since the lateral compressibility modulus of erythrocyte membranes is about equal to that of lipid bilayers (Hochmut et al. 1979), the reduced surface tension $\tilde{\gamma}$ is expected to exhibit the same value as for vesicles, namely $\tilde{\gamma} \approx -2.3$ (Duwe et al. 1989). From these data one would expect a value of $W \approx 18$.

As follows from Fig 3 b the theoretical curves $K(t)$ exhibit a non-exponential decay. This shows that the non-exponential behavior of the experimental correlation function is not a consequence of the transition between independent and peristaltic modes (Brochard and Lennon 1975), but can be explained in terms of the superposition of contributions $K_l(t)$ of individual modes. Comparison of the relative amplitudes of the fast and the slow decay of $K(t)$ shows that the best agreement between experimental and theoretical curves is obtained for $W \approx 0$. We therefore conclude that the spontaneous curvature does not markedly affect the membrane undulations. It should be noted, however, that the $l=2$ mode could be so strongly suppressed that the long time behaviour of $K_l(t)$ is determined by the $l=3$ modes which are not so strongly influenced as the former mode. A more detailed study on this problem is in progress.

3. *Influence of membrane shear elasticity*

It has been argued that the shear elasticity of the erythrocyte membrane is negligible since it is a fourth order effect (Brochard and Lennon 1975). However following Peterson (1985) the mean square amplitude is in the order of

$$\langle u_{l,m}^2 \rangle \cong \frac{k_B T}{K_c l^4 + 2\mu R_0^2} \tag{13}$$

where μ is the shear elastic modulus. Since $\mu = 6 \times 10^{-6}$ N/m (Engelhardt and Sackmann 1988; Evans and Skalak 1980) the membrane undulations would become unobservable if they would imply substantial shear deformations. Membrane shearing would also exert a strong influence on the decay constant $\omega_{l,m}$ of $K(t)$ which is approximately given by

$$\omega_{l,m} \cong \frac{1}{R_0^2} \frac{K_c l^4 + 2\mu R_0^2}{2\eta_m + \eta R_0} \tag{14}$$

where η_m is the 2 D membrane viscosity.

Since $\eta_m = 3.4 \times 10^{-7}$ Ns/m (Engelhardt and Sackmann 1988) one obtains $\eta_m \approx 20 \eta R_0$. With increasing contribution of membrane shearing, the relaxation of the undulations would be more and more determined by energy dissipation in the membrane, that is $\omega_{l,m}$ would decrease. As we will show below many effects on the flicker spectra can be interpreted in terms of shearing effects.

Results and discussion

With the methods described in the Theoretical Background Section (3) and (4) and the Appendix, relative values of the average light intensity I_0, the cytoplasmatic viscosity η and bending stiffness K_c were simultaneously measured as a function of various physical, physiological and biochemical manipulations. These can be performed by exchanging the buffer between the measurements. Individual, single cells were studied as a function of time in order to evaluate their response to the external perturbations. The main advantage of the present measuring procedure as compared to the previous study (Fricke et al. 1986) is that by simultaneous measurement of the light intensity I_0 the shape changes can be monitored. Accord-

ing to the quasi-spherical model (12a) and (12b), the viscoelastic parameters η and K_c are combinations of the true values of η' and K_c' and the equivalent radius R_0. In the following figures all parameters are plotted on the same logarithmic scale, but in order to facilitate observation they are shifted along the ordinate. In many cases phase contrast images of the cells are presented which were taken immediately after the corresponding measurements, in order to demonstrate shape changes. In separate experiments it was found that in serum containing buffer the three parameters do not change appreciably within six hours (experiment not shown), which provides strong evidence that slight fixation of the cell by (low molecular weight) polylysine does not cause substantial changes of the membrane structure and cell shape.

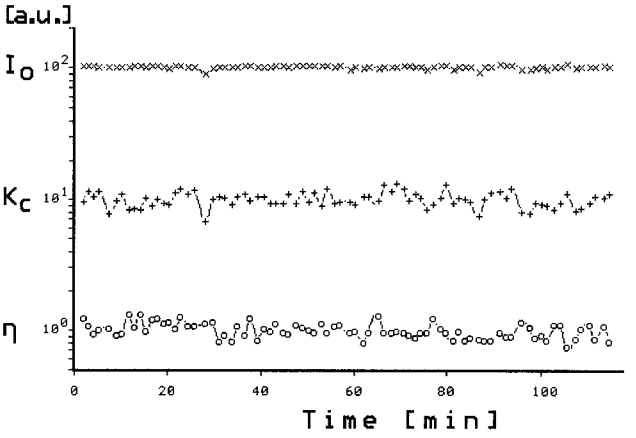

Fig. 4. Continuous measurement of I_0, K_c and η by flicker spectrum analysis of a normal cell in buffer with fetal calf serum and albumin. Measurements were performed every 1.5 min. Note: a.u. means arbitrary units

1. Temporal variation of the viscoelastic parameters

Figure 4 shows a continuous measurement over two hours. In order to test the reproducibility of the measurements of K_c and η by frequency spectrum analysis we measured these parameters repeatedly for a single cell at the shortest possible time intervals of about 1.5 min. As follows from Fig. 4 K_c and η oscillate substantially about the average value with standard deviations of 13% and 12% (and 3% for I_0) respectively. These variations limit the accuracy of the measurements. Concerning their origin in two explanations come to the fore: Firstly, they could be caused by the inaccuracy of the measurement brought about (*1*) by too short measuring times (*2*) by deviations of the measuring beam from the cell center and (*3*) by a restricted lateral Brownian motion of the only slightly fixed cells. Owing to the strong variation of I_0 (x) along a section through the cell center (cf. Fig. 3b) such a lateral jitter would indeed lead to strong variations of the measured parameters. Secondly, these temporal variations could be caused by real random oscillations of K_c or the cell volume.

2. Effects of the volume of the cells

Figure 5 shows the variation of the parameters I_0, K_c and η with the osmolarity of the buffer and therefore with the volume of the cell. The degree of shrinking at increasing osmolarity is clearly indicated by the increase in I_0. Between 200 and 300 mosm both the bending elastic modulus K_c and the viscosity η decrease drastically. While K_c decreases further (although less rapidly) up to 420 mosm, η starts to increase strongly at 300 mosm. Remarkably, the increase in I_0 is saturated at the same osmolarity ($\approx$420 mosm) where K_c starts to increase again. Since the data in Fig. 5 were obtained from different cells they show universal behavior of erythrocytes. The behavior of K_c and η can be largely understood on the basis of the quasi-spherical model. Consider first the region between 200 and 260 mosm. Since R_0 changes only by 10% it cannot account for the large increase of K_c and η with decreasing osmolarity. These increases can be explained by the influence of the surface tension γ which, according to (7), reduces in particular the amplitude of the lowest order mode ($l=2$) and thus causes an increase of the apparent K_c and η (cf. (12) for definition of apparent K_c-value). In principle values of γ could be determined as a function of swelling of the cell. But since an accurate value of the spontaneous curvature w is not known yet these data on γ would be at most order of magnitude estimations.

K_c decreases further with increasing osmolarity (up to 450 mosm). As noted above, the shape fluctuations of the cell can be explained in terms of spherical harmonic excitations about the rotational symmetry axis of the cell. Since the diameter of the cell increases with increasing deflation (photograph Fig. 4) the effective equivalent radius R_0 becomes larger too. It is most likely for that reason that the apparent K_c ($K_c = K_c'/R_0^3$) decreases with osmolarity cf. (12b). The sharp rise of K_c at 450 mosm which is accompanied by the saturation of the increase of I_0 is attributed to the mutual interaction of the two opposing membrane skeletons. The increase of the viscosity η by a factor of ten between 300 and 500 mosm reflects the increase of the viscosity of the cytoplasm by dehydration as well as the interaction of the cytoskeleta.

3. Membrane excitations of camel erythrocytes

The camel erythrocytes exhibit an elliptic cross-section of 8–10 μl length and 5–6 μm width and are bulged out in the center to a thickness of about 2 μm (cf. Fig. 6). Blood of Camelus dromedarius was provided by Dr. von Hegel from Tierpark Hellabrunn (Munich) and the cells were diluted in the buffer with serum. Figure 2d shows a typical frequency spectrum taken at 300 mosm. The quantitative evaluation shows that compared to human cells the intensity I_0 is reduced by a factor of three (due to the cell shape), whereas the viscosity η and the bending modulus K_c are increased by a factor of twenty and four, respectively. The integrated spectrum $\int P(\omega)\, d\omega$ is reduced by a factor of five. The reduced flickering as compared to human cells can be attributed to the very rigid membrane of the camel cell which has a high protein to lipid ratio of 9 to 1 in the lipid/protein bilayer. The content of protein

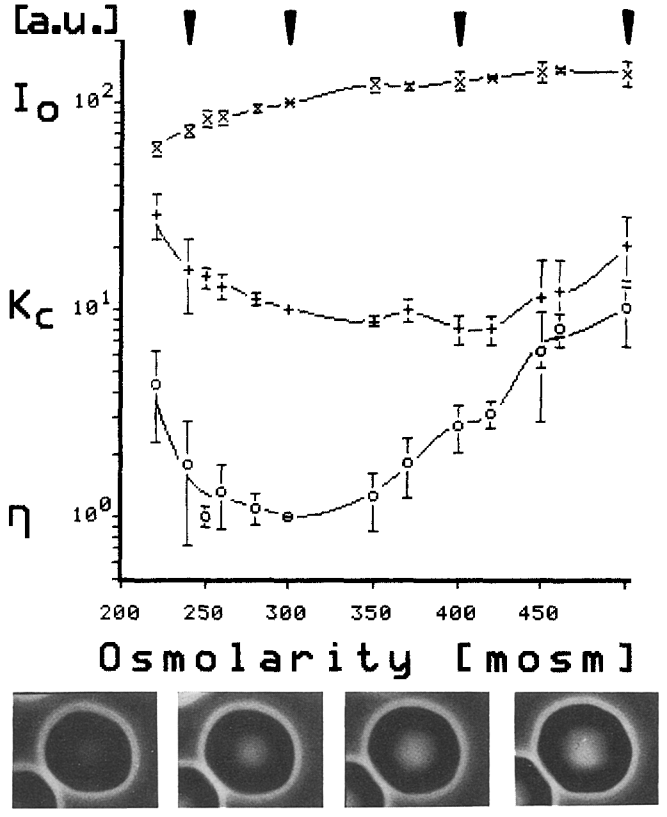

Fig. 5. Variation of the average intensity I_0, the viscosity η ($=\eta' R_0$, Eq. (12a)) and the bending modulus K_c ($=K_c'/R_0^3$) with osmolarity of medium. The ordinate is in the same logarithmic scale for all parameters which are (for clarity) mutually shifted vertically in such a way that for the physiological osmolarity (300 mosm) the values of I_0, K_c and η are 10^0, 10^1 and 10^2 respectively. For each osmolarity the parameters were measured for several (two to eight) different cells. The vertical bars show the variances of these values. At the bottom, images of one of the cells are given at the osmolarities indicated by the arrows on the top of the figure

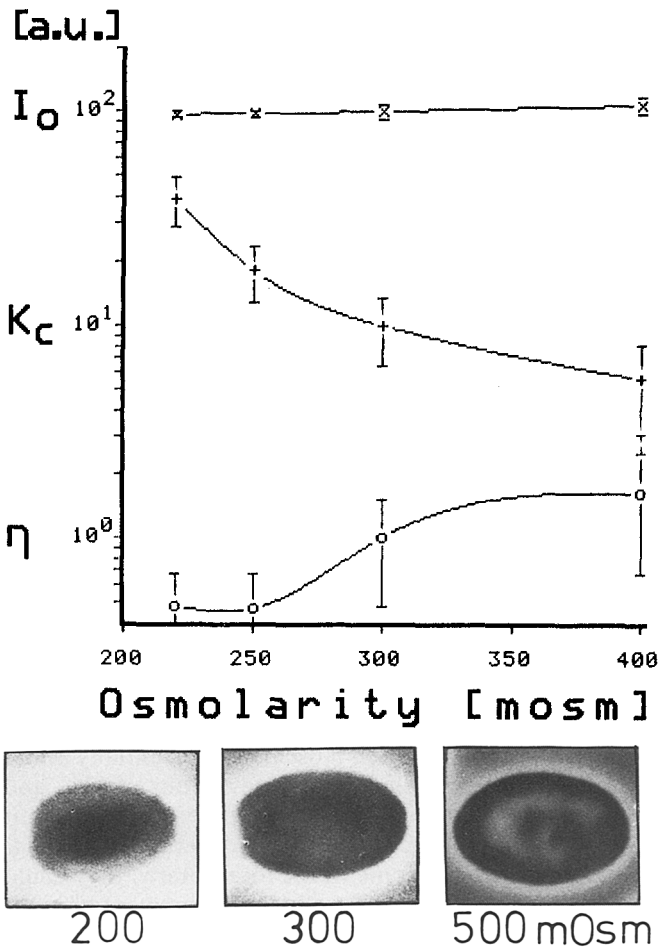

Fig. 6. Flickering of camel erythrocytes. Variation of the parameters I_0, K_c and η (on relative scale). Each value is the average of the measurements of 3 cells. The phase contrast micrographs show camel erythrocytes for 200, 300 and 500 mosm. Note the buckling of the cell at 200 mosm

Band III is higher than that of human cells and the coupling of ankyrin to the bilayer is enhanced (Khodadad and Weinstein 1983). However, it could also be caused by the much larger shear rigidity. The shear elastic modulus of the camel erythrocyte membrane is drastically enhanced as compared to human cells. Therefore they cannot be deformed in the electric field (Engelhardt, unpublished results) or in the hydrodynamic shear field (Smith et al. 1979). Figure 6 shows the variation of I_0, η and K_c with the osmolarity. The most interesting feature is the increase of K_c by a factor of about six between 400 and 220 mosm and the simultaneous decrease of η. This opposite behavior of the two parameters contrasts with the finding for human cells (Fig. 5). The very strong increase of K_c is attributed to the tension arising during the swelling. Evidence for this comes from the remarkable finding that the cell starts to buckle below 220 mosm as can be clearly seen in Fig. 6. Below 220 and above 400 mosm the undulations become too weak to be evaluated. The camel cells show a remarkable stability of shape with respect to calmodulin inhibition by triflouperazine: a cup-building agent (cf. below). Even at 10 μM triflouperazine they do not change their shape but K_c and η are reduced by about 40%.

4. Effects of shape changes

In Figs. 6 to 9 we present some examples which show the effect of shape changes on the membrane undulations. The reversibility of such effects as well as remarkable transient shape transitions are shown.

Examples of Cup-formation

Cup-formation induced by triflouperazine (Fig. 7a): This is an example for a rapid shape change. The parameters I_0, η and K_c are recorded as a function of time while the cells are incubated with different concentrations of triflouperazine (purchased from Sigma). 5 μM triflouperazine increases I_0 and K_c by 50% and η by 100%. The change of the parameters is reversed after rinsing the cells with pure buffer. As reported by Nelson et al. (1983) triflouperazine induces a discocyte-stomatocyte transition. This is in agreement with our finding: after addition of the agent I_0 increases strongly owing to this shape change. The experiment leads to the conclusion that cup-formation increases η much more than K_c. A similar behavior of the measured parameters has been observed in the case

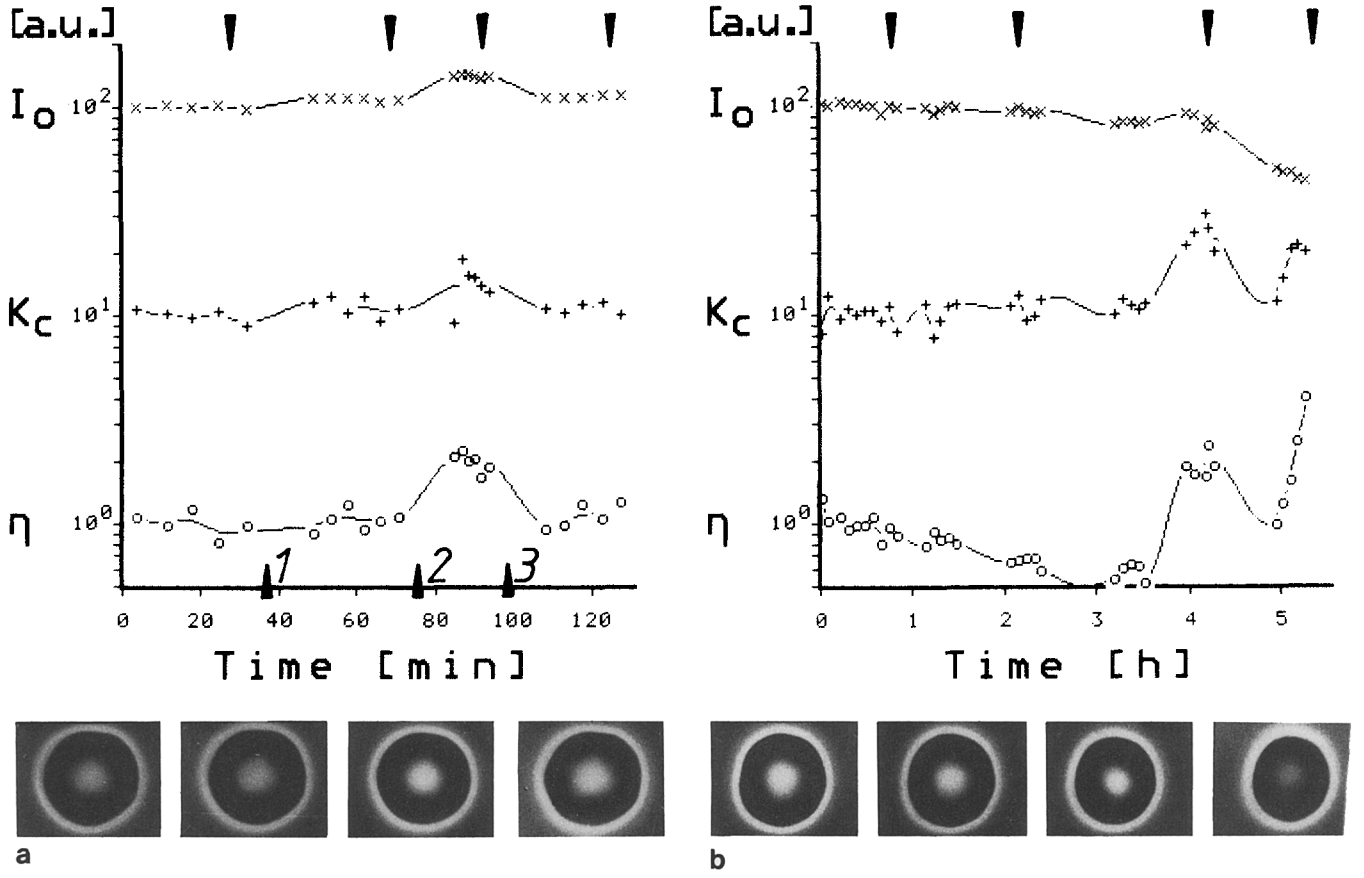

Fig. 7. Effects of spontaneous (**a**) and delayed (**b**) cup-formation of cell on the parameters I_0, K_c and η. **a** cup formation caused by 0.5 μM (↑1) and 5 μM (↑2) triflouperazine. The shape change is reversible after rinsing with pure buffer (↑3) (buffer with serum). Phase contrast images of the cell were taken at the times indicated by arrows (↓). **b** Storage of a cell in the buffer containing only albumin (2.5 mg/ml). Before starting the measurement the cells has been pre-incubated for two hours as usual

of the deflation of the cell (cf. Fig. 5). It is then difficult to distinguish between these two shape changes.

Cup-formation induced by storing in buffer without serum (Fig. 7b): This is an example of a delayed shape change which is caused by aging of the cell in the buffer containing only albumin. One observes a superimposition of a continuous swelling and a transient cup formation at $4<t<5$ h. Three time regimes may be discerned in Fig. 7b. In the first 3.5 h I_0 and η decrease continuously while K_c increases very slightly. This is certainly an effect of swelling which has been attributed to a Na^+-influx into the cell. A possible explanation for the increased ion-permeability of the membrane is the removal of lipid from the lipid/protein bilayer by the glass surface of the measuring chamber (Shohet and Nathan 1970). Comparison with Fig. 5 shows that the swelling would correspond to an increase in osmolarity from 300 to 250 mosm. After 3.5 h, I_0 increases slightly and K_c and η more drastically, namely by factors of four and six, respectively. This change is transient since after 5 h, K_c and η nearly regain their previous values. The increase of I_0 during the transient change of K_c and η points clearly to cup-formation. Finally, that is between 5 and 5.5 h, the cell swells rapidly. The concomitant increase in K_c and η is attributed to the lateral tension arising during the swelling. This temporal behavior has been observed for two out of three cells measured. The transient discocyte-to-stomatocyte transition has also been found in spherocyte-formation caused by ATP-depletion by iodoacetate (experiment not shown) and thus appears to reflect an universal behavior of erythrocytes during swelling.

Examples of echinocyte-formation

The effects of two different types of discocyte-echinocyte transitions on the viscoelastic parameters K_c and η are shown below (cf. Fig. 8).

Incubation with DMPC-vesicles (Fig. 8a): In this experiment the cells (fixed to the glass plate of the measuring chamber) are incubated with a suspension of vesicles of dimyristoylphosphatidylcholine (DMPC) in buffer. 0.5 mg DMPC (purchased from Sigma) were sonicated in 1 ml buffer in a bath sonicator for 15 min at temperatures larger then 30 °C (Ott et al. 1981). Since the vesicles scatter light strongly the cells were preincubated only for 10 min with the vesicle suspension and then rinsed again by pumping pure buffer into the chamber. After this preliminary treatment the measurements in Fig. 8a were started. I_0, η and K_c decrease continuously, while the cell

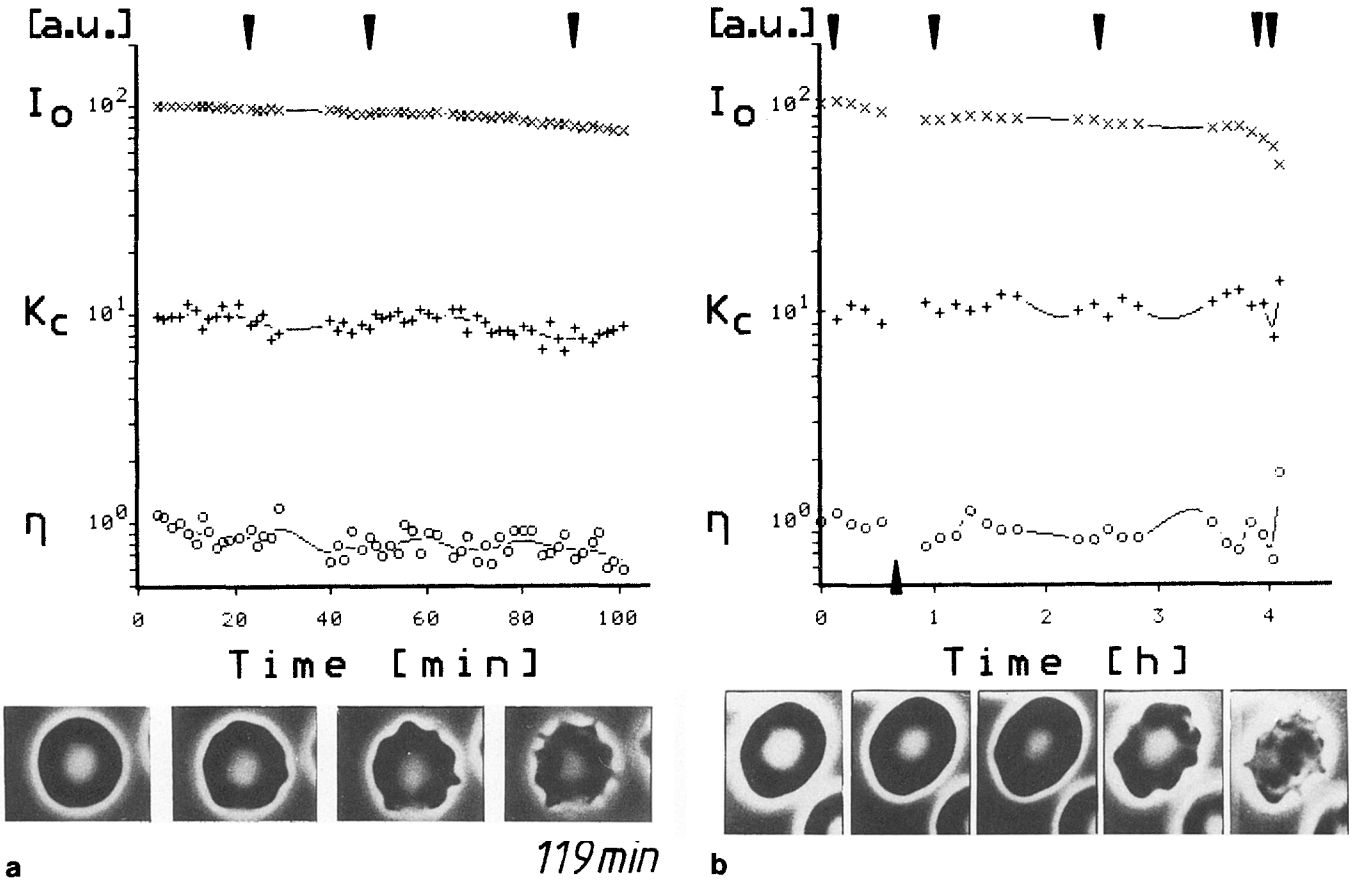

Fig. 8. a Variation of parameters I_0, K_c and η induced by incubation of the erythrocytes with a DMPC-vesicle-suspension (0.5 mg/ml) in buffer with serum. Prior to the start of the measurement the vesicle suspension was pumped into the chamber for 10 min only and then removed again to avoid light scattering effects. Enough lipid remains in the chamber to induce the shape transition. The phase contrast micrographs show the cellular shape at the times indicated by the arrows. **b** Effect of ATP-depletion after rinsing the cell with physiological NaCl solution. The cells are first incubated in buffer (with serum) and transferred into the measuring chamber. The NaCl solution is added at the time indicated by the arrow (↑). Phase contrast images of the cell were taken at the times indicated by arrows (↓)

becomes echinocytic. The decrease in I_0 is certainly not caused by a swelling of the cell, because then (according to Fig. 5) K_c and η would have to increase owing to the surface tension effect. Therefore we conclude that the cell makes a transition towards a sphero-echinocyte without volume change. Furthermore this seems to be accompanied by an increase of the area of the lipid/protein bilayer by lipid incorporation. It has indeed been shown by Ott et al. (1981) that the PC content of the membrane increases by about 150% by incubation with DMPC-vesicles. Evidence for an increase of the bilayer area is also provided by the formation of sharp spicules (cf. photographs Fig. 8 a) formed by the excess area.

Storing in physiological NaCl-solution (Fig. 8 b): A discocyte-echinocyte transition caused by incubation in physiological (155 m*M*) NaCl-solution in shown in Fig. 8 b. This shape change is attributed to ATP depletion of the cell owing to the high activity of the ion pumps. The passive ion-permeability of the cell membrane is strongly enhanced in the NaCl-solution devoid of protecting proteins, in particular if the cells are in addition fixed to the bare surface of the chamber. The enhanced consumption of ATP cannot be compensated by its resynthesis owing to the lack of dextrose in the medium. The remarkable result of the flicker spectrum analysis is, that K_c and η remain essentially constant although the shape changes towards a spheroechinocyte.

Both experiments of Fig. 8 show that echinocytes may exhibit the same low bending stiffness as normal discytes, that is the spicule formation has a small influence on the flickering amplitude. This provides strong evidence that the spicules can act as area reservoirs for the membrane undulation.

5. *Modulation of bilayer-cytoskeleton coupling*

Coupling of bilayer and cytoskeleton by WGA. Figure 9 a shows the change of the three parameters (I_0, η, K_c) caused by various amounts of wheat germ agglutinin (WGA), a lectin from *Triticum vulgaris* (purchased from Sigma). This agent has been dissolved in the buffer (with serum) at the three concentrations given in the insert of Fig. 9 a. The three solutions where added in sequence at intervals of 30 min. The intensity I_0 increases slightly (by 30% at a concentration of 1 μg/ml) which could be due either to a deflation of to a slight cup-formation of the

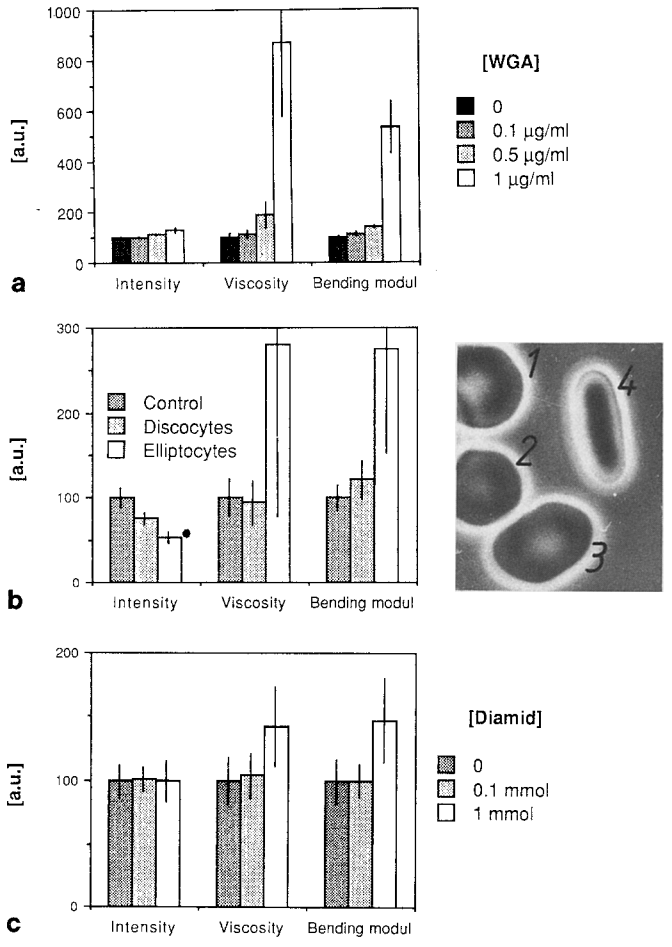

Fig. 9. **a** Effect of wheat germ agglutinin (WGA) on the parameters I_0, K_c and η, measured by correlation function analysis in buffer with fetal calf serum. For each concentration of WGA the parameters are measured 6 times for two different cells. The values given are averages over these measurements. The values are given in relative units which are set to 100 for the control cells, the variances are indicated by the vertical bars. **b** Normal shaped and elliptic erythrocytes of patients suffering from elliptocytosis are compared with control cells. 15, 4 and 20 cells were measured by frequency spectrum analysis in buffer with fetal calf serum. The phase contrast image shows the two types of erythrocytes (1 and 2 normal shaped cells, 3 and 4 elliptic cells). The average values I_0, K_c and η of the control cells are set to 100. **c** Effect of 0.1 mM and 1 mM diamide on the parameters I_0, K_c and η, measured by correlation function analysis in buffer with autologuous serum. 2 µl freshly drawn blood with Na_3-citrate as anticoagulant were washed three times with physiological NaCl solution. The erythrocytes were incubated with diamide in physiological NaCl solution for 60 min at 37 °C. Than they were washed three times with the measuring buffer and stored on ice until measurement (performed within one hour). The buffer with autologuous serum has the advantage that the cells can be measured immediately. 30 to 53 cells were measured for each sample

cell (cf. experiments of Fig. 5 and 7a). However, this shape change can certainly not account for the very large increase of the viscoelastic parameters η and K_c by factors of eight and five, respectively. Obviously, WGA causes a drastic change of the membrane organization. As reported by Chasis et al. (1985) WGA leads to formation of a protein network on the cell surface and to a coupling of the glycophorin A to the cytoskeleton. The latter would correspond to a WGA induced coupling of the cytoskeleton to the bilayer and as a consequence of this an increase in the lateral tension during bending, this could indeed lead to the observed strong increase of both K_c and η.

Perturbation of bilayer-cytoskeleton coupling by diseases. The above experiment shows that the glycophorin-membrane-skeleton interaction affects the membrane deformability strongly. Further evidence for this conclusion comes from Fig. 9b which shows that the slightly elliptic population of erythrocytes from patients suffering from elliptocytosis exhibit threefold higher values of η and K_c than cells from normal donors of the normal shaped cells of the same elliptocytosis blood sample. The strongly deformed elliptic cells do not flicker and are therefore not measurable. The blood from patients with Type Gerbich Negative elliptocytosis (kindly provided by M. J. A. Tanner, Department of Chemistry, Medical School, Bristol, UK and D. J. Anstee, National Blood Transfusion Service, Bristol, UK) lack three glycoproteins including glycophorin C. It is well known, that the glycophorins A and C play an important role in the coupling of the spectrin/actin network to the bilayer via the band 4.1 protein (Steck 1989). Accordind to Takakuwa et al. (1986) the absence of the band 4.1 protein also causes elliptocytosis whereas re-injection of this protein into the deficient cells recovers the discocyte shape. It is thus the absence of this actin-band 4.1-glycophorin coupling which causes elliptocytosis. One likely explanation for the reduced flickering is the increase in shear rigidity. Indeed, the elastic shear modulus is increased by a factor of 2.8 as found by the electric field deformation technique (Engelhardt and Sackmann 1988). Another example showing the subtle control of cytoskeleton structure and elasticity by membrane glycoproteins is the variation of η and K_c by stomatocytosis. These erythrocytes (Rh_{null}-type-stomatocytosis, kindly provided by D. J. Anstee, see above and M. Bruce, Glasgow and West of Scotland transfusion Service, UK) lack blood group antigens. In this case η is increased between 50 and 100% while K_c remains essentially constant (experiment not shown). On the other hand the shear rigidity is decreased by 100% (Engelhardt and Sackmann 1988), which could explain the small change of K_c.

Crosslinking of the cytoskeleton by diamide. In surprising contrast to the above finding, the cross-linking of spectrin by diamide exerts only minor effects on the membrane undulation (Fig. 9c). The concentration of 0.1 mM diamide which drastically reduces the deformability of the cells in shear fields (Chasis 1986) has no effect on the membrane undulation and 1 mM diamide is required in order to increase K_c and η by 50%. At this concentration the shear elastic constant μ is eight-fold enhanced (Engelhardt and Sackmann 1988). According (13) and (14) it could be this increase in the shear rigidity which leads to the observed increase of K_c and η.

In summary, the coupling of bilayer and cytoskeleton (e.g. by WGA) has a strong influence on the membrane

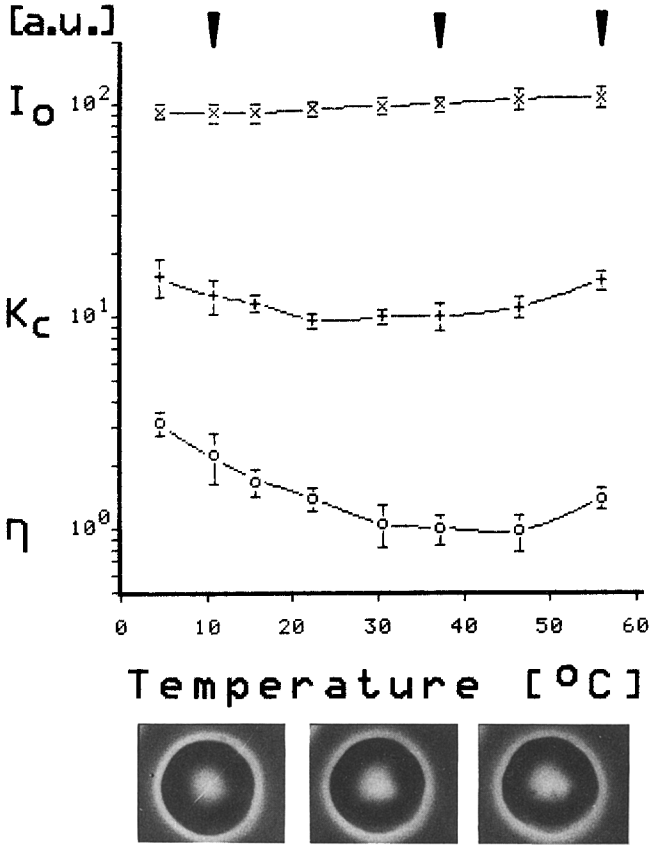

Fig. 10. Variation of parameters I_0, K_c and η by altering the temperature in buffer with serum. The temperature is adjusted with an accuracy of ± 3 °C via tempering the objective of the microscope by a thermostat (Frigostat, from Desaga, Heidelberg, FRG). The temperature is increased stepwise, the whole measurement lasts 140 min. For each temperature the parameters of three cells were measured twice, the bars show the variance of these values

undulation due to the lateral tension arising during bending. Crosslinking of the cytoskeleton (e.g. by diamide) enhances the shear rigidity strongly, but has only a minor influence on membrane undulation.

6. Temperature dependence of the flickering

Figure 10 shows the change of the viscoelastic parameters with the temperature. The brightness I_0 of the cells increases during heating which points to a slight shrinking or cup-formation. The viscosity η of the cytoplasm decreases with temperature as expected. The bending elastic modulus K_c exhibits a broad minimum between 20 and 40 °C. The increase of K_c at temperatures <20 °C is attributed to a conformational change of the lipid bilayer (Kapitza and Sackmann 1980). At temperatures >50 °C both K_c and η are enhanced which could be due to a loss of the membrane deformability owing to membrane protein denaturation (Yoshino and Minari 1987). The cells did not fragment within the time of observation of some 10 min in contrast to the study of Deeley and Coakley (1983). One reason for this high stability may be the presence of serum.

General discussion

1. Estimation of the absolute bending modulus K_c from the decay rate of the correlation function using the quasi-spherical model

The analysis of erythrocyte flickering in terms of the quasi-spherical model allows us to differentiate between effects of changes of the volume and shape and true modifications of the membrane. This is not possible in the plane wave model used previously (Fricke et al. 1986). A quantitative evaluation in terms of the quasi-spherical model is, however, certainly only possible for the biconcave shape at moderate degrees of deflation ($\leq$250–400 mosm). The model accounts in particular for the non-exponential decay of the intensity autocorrelation function. Since the long time behavior is determined by the lowest order mode, the corresponding reciprocal correlation time of $\tau^{-1} \approx 6\ s^{-1}$ (cf. Fig. 3b) is about equal to ω_2 (cf. 10). One obtains from (10) and for $(\tilde{\gamma}+4w-2w^2) \approx 1$ $K_c \approx 2.5\ R_0^3 \eta$ (cf. text to Fig. 3b). The viscosity of the cytoplasm is $\eta = 6 \cdot 10^{-3}$ Nm^{-2} and for $R_0 = 2.9$ µm (at 300 mosm, Canham 1970) one finally obtains $K_c = 2-3 \cdot 10^{-19}$ Nm. This is nearly an order of magnitude larger than the average value of $K_c = 3.4 \cdot 10^{-20}$ Nm obtained from the mean square amplitude measurements by RICT (Zilker et al. 1987). The above value is, however, only an estimate of the upper limit of K_c since the lowest order mode depends most critically on the poorly known parameters $\tilde{\gamma}$ and w. The average value obtained by RICT is mainly determined by the high order modes and indeed yields a value of $K_c \approx 10^{-19}$ Nm if only the longest wavelength mode is considered. In summary, the bending stiffness of the cell as determined in this work and previously (Zilker et al. 1987) appears to be too small, considering the high cholesterol content of 50 mole% of the bilayer. For DMPC bilayers containing 30 mole% cholesterol we found a value of K_c' of $5 \cdot 10^{-19}$ Nm compared to $1.2 \cdot 10^{-19}$ Nm for pure DMPC (Duwe et al. 1989). The low value of the bending elastic modulus K_c is in particular interesting in view of the shear elasticity of the membrane which according to (13) and (14) should cause a further increase in the apparent K_c value of erythrocytes. This provides evidence that the cell exhibits a shear free regime of deformation, a point which is further discussed below.

2. Universal behaviour of human erythrocytes

The strategy followed in this work has been to measure the temporal changes of the parameters I_0, η and K_c of single cells caused by physical or biochemical perturbations. The aim was to find universal features in the cellular response despite the large variability within the same cell population. By measuring the parameters I_0, η and K_c of 45 cells we found variances of 12%, 28% and 21% respectively. Some universal features are:

1. The apparent bending stiffness K_c of biconcave cells is well controlled over a large range of osmolarities (250–450 mosm) whereas the apparent viscosity η has a mini-

mum at physiological osmolarity. Interestingly K_c and η are also minimal in the physiological temperature regime (cf. Fig. 10).

2. The values of K_c and η do not increase significantly even in the case of echinocyte formation e.g. by ATP depletion in NaCl solution (cf. Fig. 8 b) or by expanding the bilayer by addition of DMPC (cf. Fig. 8 a). This suggest that the spicules can follow the slow motion of the $I=2$ mode exhibiting a relaxation time of about 0.2 s.

3. Two requirements for the maintenance of strong flickering appear to be essential: firstly, the preservation of a shear free deformation regime of the cytoskeleton and secondly the absence of surface tension. The former condition is certainly lost in the case of crosslinking of the cytoskeleton by SH-ligands (diamide), the second condition is lost for osmotic swollen cells.

4. The state of coupling of bilayer and cytoskeleton influence the membrane undulations strongly. Coupling (e.g. by WGA) probably increases the lateral tension within the membrane during bending.

5. The strong and rather abrupt increase of the apparent η and K_c after complete deflation of the cell (≤ 450 mosm) is certainly not only a consequence of the enhanced viscosity of the cytoplasm but has to be also attributed to the mutual interaction of the two opposing cytoskeleta. Because the two membranes can only undulate collectively in this case a high lateral tension arises during bending which would increase the apparent η and K_c.

6. Even slight cup formation enhances η and K_c drastically where η is most strongly affected (Fig. 6). This is certainly partially due to the effect of the surface tension $\tilde{\gamma}$. But cup formation is also associated with an increase in negative spontaneous curvature w, which increases η and K_c in the same way as $\tilde{\gamma}$. In those cases where cup formation is caused by an expansion of the cytoskeleton it could also imply the loss of the shear free deformation regime. Unfortunately the present flicker technique does not allow us to separate the latter (and most interesting) mechanism from the shape effects.

3. Induced shape transitions

In the present work induced shape changes were mainly of interest regarding their effect on the flickering. It has become evident that the shape changes can be explained in terms of induced bending moments (or spontaneous curvature) (Svetina and Zeks 1989) as originally proposed by Evans (1973) and Deuling and Helfrich (1976) and verified experimentally for erythrocytes by Sheets and Singer (1974) and for model membranes by Duwe et al. (1987). The plane of attack of the bending moment may be located in any of the three layers of the cell envelope: the glycocalix, the bilayer and the cytoskeleton. Thus an induced curvature could be caused (*1*) by lateral pressure within the highly charged glycocalix alone, (*2*) by a mutual change in area between the two monolayers of the lipid/protein bilayer (corresponding to the bilayer coupling hypothesis of Sheets and Singer (1974)) and (*3*) by expansion or contraction of the whole lipid/protein bilayer with respect to the membrane skeleton. The initial albumin-induced cup-formation belongs to the first two mechanisms. It is not clear yet whether it is due to a contraction of the glycocalix or to the extraction of fatty acids or short chain lipids from the outer lipid monolayer or the glycocalix. The former effect could also be caused by a change of the ionic strength or by dehydration of the glycocalix. Since this is an osmotic effect the albumin does not have to adsorb to the membrane surface. Shape changes – such as the discocyte-stomatocyte transition – may also be induced by mechanical instability (buckling, Evans 1973). A potential example is the (probably albumin induced) transient cup formation during swelling presented in Fig. 8 b. An example of a shape change induced by variation of the bilayer area is the echinocyte formation induced by incubation with DMPC-vesicles (Fig. 8 a). The lipid is first incorporated into the outer monolayer, then excess lipid is transferred into the inner monolayer.

4. Excess bilayer area model of a shear free (dynamic) deformation regime

Two features of the red cell membrane are suggested by the present study: (*1*) The bending modulus K_c is smaller than expected considering the high cholesterol content of the bilayer. (*2*) The cytoskeleton must exhibit a shear free deformation regime. In the following we suggest that the above features may be explained in terms of a metastable state of coupling of the network to the bilayer and a slight excess area of the bilayer with respect to the cytoskeleton resulting in a locally undulated surface. The combined effort of many groups (cf. Steck (1989) for reference) has led to the present image of the cytoskeleton structure and its coupling to the lipid/protein bilayer which is shown in Fig. 11. Many (but certainly not all) of the essential elements of the network are known and most of them have one or more phosphorylation sites (Backman 1988). These elements include: spectrin ($1 \cdot 10^5$ tetramers per cell, 8–10 phosphorylation sites); actin ($3–4 \cdot 10^4$ oligomers of 35 nm length per cell, stabilized by a tropomyosin dimer; no phosphorylation sites); protein band 4.9 ($4 \cdot 10^4$ trimers per cell, 8 phosphorylation sites); protein band 4.1 ($2 \cdot 10^5$ monomers per cell, unknown number of phosphorylation sites); ankyrin ($1 \cdot 10^5$ monomers per cell, unknown number of phosphorylation sites); protein band III ($2.5 \cdot 10^5$ tetramers per cell, unknown number of phosphorylation sites); Glycophorin A ($2 \cdot 10^5$ species per cell) and Glycophorin C ($5 \cdot 10^4$ species per cell). As suggested by the elegant electron microscopic studies of Triton X-100 isolated skeletons (Shen et al. 1984; Byers and Branton 1985; Liu et al. 1987) the network exhibits on the average a triangular lattice. The bonds consist of the spectrin tetramers and the vertices are formed by the actin complexes (Bennett 1989; Steck 1989). These act as multifunctional crosslinks to which the spectrin tails are connected most probably via band 4.1. As pointed out in particular by Liu et al. (1987), many of the vertices have 5-fold and 7-fold symmetry. From the point of view of triangular lattice

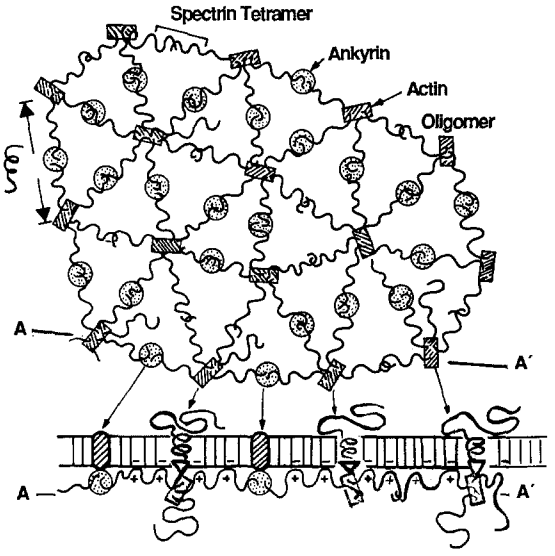

Fig. 11. Schematic view of the quasi-two-dimensional spectrin-actin network as suggested by electron microscopic studies of Triton isolated skeletons (cf. Steck 1989). On the average the network forms a triangular lattice with spectrin-tetramers forming the bonds (with an estimated length of $\xi = 68$ nm) and actin complexes (consisting of ≈ 13 actin monomers and a tropomyosin dimer) forming the vertices. The coupling of the network to the lipid/protein bilayer is mediated (*1*) by ankyrin which attaches the spectrin tetramer (bivalent head-to-head cross-links of two spectrin dimers) to band III and (*2*) by band 4.1 (not shown) which attaches the actin complexes (= vertices) to a membrane glycoprotein, namely glycophorin C and according to Bennett (1989) also to the band III protein. The band 4.1 binding site for glycophorin is highly hydrophobic (Mohandas, private communication) and may thus penetrate deeply into the bilayer. The band 4.1 protein stabilizes simultaneously each of the spectrin-actin cross-links. The network exhibits a large number of defects, that is vertices with 5- and 7-fold cross-links. The former corresponds to $+60°$ and the latter to $-60°$ disclinations of a triangular lattice. Two of such disclinations may form pairs or may dissociate. In the latter case the network is expected to be very soft with respect to shearing (Nelson and Halperin 1979)

topology these correspond to $-60°$ and $+60°$ disclinations (Nelson and Halperin 1979). By assuming that all $(1 \cdot 10^5)$ spectrin tetramers take part in the network formation one can estimate the average bond length $\langle L \rangle$ per spectrin tetramer required to form a triangular network of the given area A of an erythrocyte. The number of the (equilateral) triangles n_t, the bonds n_b and the (6-valent) vertices n_v for a triangular network are:

$$n_t = \frac{4A}{\sqrt{3}\langle L \rangle^2} \qquad n_b = \frac{3}{2} n_t \qquad n_v = \frac{1}{2} n_t \tag{15}$$

Now, the average area of the cell membrane is $A \approx 140\ \mu m^2$ (Canham 1970). It thus follows that to form $1 \cdot 10^5$ bonds the average-bond length must be $\langle L \rangle = 68$ nm. The corresponding number of triangles is $n_t = 7 \cdot 10^4$ and of vertices $n_v = 3.5 \cdot 10^4$. The latter value is slightly smaller ($\approx 10\%$) than the average number of actin oligomers present in the cells. It agrees however, very well with the number of glycophorin C molecules, the anchors for the vertices. In electron microscopic studies of the Triton extracted cytoskeleton the length of the completely expanded spectrin tetramer has been estimated to be 200 nm. As one knows from dynamic light scattering studies of spectrin in solution, the dimers from random coils of ellipsoidal shape with a hydrodynamic length of the long axis of about 33 nm (Egglestaff, unpublished results obtained in authors laboratory) which agrees well with half the bond length estimated above. This suggests that spectrin assumes a nearly relaxed configuration within the network which allows contraction and extension and is thus expected to be flexible enough to allow strong thermally driven undulations. It is interesting to note that the random coil like structure of spectrin is also suggested by measurement of the thickness of the cytoskeleton of 60 nm by Bull et al. (1986). Both elements of the composite membrane, the membrane skeleton and the bilayer must undulate collectively. This implies two problems: firstly, as noted above, the high cholesterol content of the bilayer is hard to reconcile with the observed low bending modulus and secondly, owing to the large thickness (of some 60 nm) of the composite membrane the undulations are expected to be associated with large local lateral tensions. The above constraints could, however, be relaxed by any of the following mechanisms or a combination of these: (*1*) by a very loose coupling of the network to the bilayer allowing for a fast mutual shift of the two sheets and (*2*) by creation of an excess area of one sheet of the composite membrane with respect to the other. Consider the first possibility: It has been found by several authors (cf. Cohen and Foley (1980) and Bennett (1989) for reference) that in their phosphorylated states the coupling proteins ankyrin and band 4.1 bind much weaker (at least in vitro) to band III and actin oligomers than if dephosphorylated. Under normal conditions the network may thus only be coupled to the bilayer at a few (non-phosphorylated) sites whereas the bulk of the vertices are so weakly interacting (possibly via Coulomb forces) that the bilayer and the network may freely slide mutually. Concerning the second possibility there is some evidence from freeze fracture electron microscopic studies of intact erythrocyte membranes. These exhibit a slight undulation of the bilayer as follows from the speckle-like variation in thickness of the platinum shadow in the example shown in Fig. 12b. This undulation has been observed in practically all cases studied but is never seen in the case of fluid vesicles. This suggests that the area of the bilayer of the erythrocytes is slightly larger than that required to span the surface of the cytoskeleton. The average wavelength of the undulations is about 100 nm (and thus about equal to the mesh size of the cytoskeleton), the amplitude is of the order of 10 nm. The thermal excitations of such a shell would only be determined by the bending stiffness of the cytoskeleton provided the bilayer could rapidly expand or contract by local flow; either by (directed) diffusion of the membrane proteins to which the network is bound or by sliding of the points of contact along the bilayer-cytoskeleton interface. The protein diffusion coefficients are $\approx 10^{-9}$ cm^2/s (Golan and Veach 1980) which allows a diffusion over distances of 200 to 500 nm within the observable response times of the undulations of 0.1 to 0.2 s. But since the latter decreases with the third power of the wave vector the lipid bilayer is expected to determine the undu-

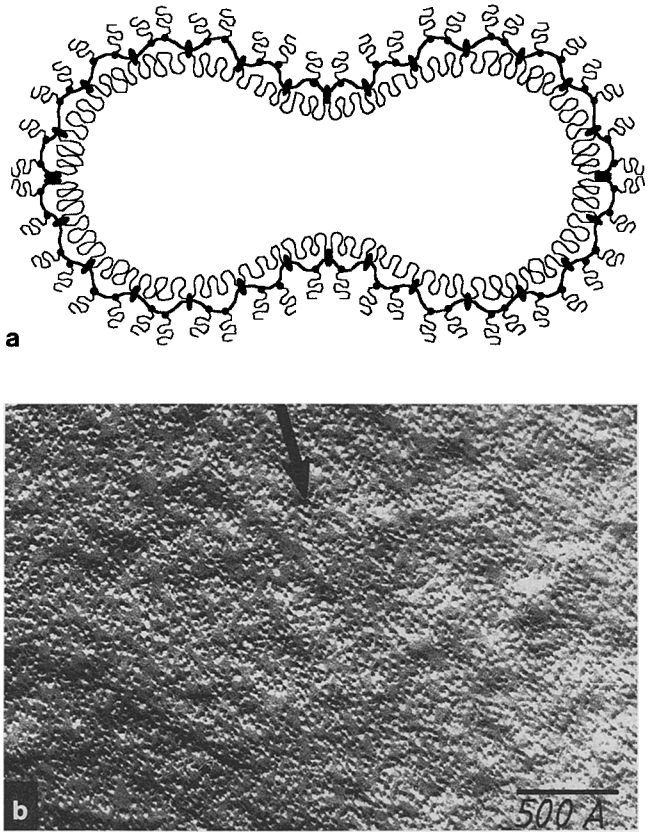

Fig. 12. **a** Excess bilayer are model of the erythrocyte membrane. A small excess of the area of the bilayer (over the value required to cover the network) is compensated by a small undulation with wavelengths of some 100 nm. Only a fraction of the bilayer-cytoskeleton contact points may be strongly coupled (for instance by ankyrin and band III). Note that the undulations may lead to a non-random distribution of membrane proteins, that is glycophorin C is expected to be accumulated in regions of positive curvature owing to head group repulsion (Petrov et al. 1979). **b** Freeze fracture electron micrograph of erythrocyte membrane (inner monolayer exhibit) of rapidly (that is by jet) frozen cells. Rotational shadowing under angle of incidence of the platinum beam of 45°. The thick arrow indicates shadowing direction. Note that the platinum layer varies in thickness indicating a slightly undulated surface of a wavelength of about 100 nm

lation amplitudes at short wavelengths. This could be one reason for the apparent increase of K_c observed by the RIC-technique (Zilker et al. 1987) at wavelengths below 0.5 μm. The idea that the bilayer surface area exceeds that of the tension-free skeleton was expressed also in the review by Steck (1989). This conjecture is based on the finding of a smaller size of the membrane skeleton isolated in physiological saline solution compared to the dimension of the parent cell.

Concluding remarks

The major conclusions of the present work are: (*1*) the membrane undulations are determined by the flexural rigidity of the spectrin/actin network which exhibits a shear free deformation regime. (*2*) The lipid/protein bilayer does not markedly limit the excitation amplitudes (at least at long wavelengths) owing to a small excess area implying a locally undulated surface profile. (*3*) The undulations are not restricted by spontaneous curvature effects. (*4*) The bending stiffness of the membrane is determined by the topology of the network and the number of sites of strong bilayer-network coupling and (*5*) the band 4.1 plays a decisive role in this coupling. (*6*) K_c and η are minimal in the physiological osmolarity and temperature regime and the cell is able to maintain this optimum even under prolonged environmental stress. It cannot be decided yet whether the undulations are purely thermally driven. Chemically induced bending moments (e.g by random phosphorylation-dephosphorylation reactions) would yield the same flicker spectrum. As pointed out previously (Fricke et al. 1987), the undulations could also be driven by lateral density fluctuations of the network, for instance induced by fluctuations in ion concentrations (e.g. Ca^{++} and K^+ etc.).

It should be pointed out that the flicker analysis gives insight into the elastic properties within a small (and dynamic) deformation regime of the membrane and thus allows only restricted conclusions concerning the correlation between membrane structure and mechanical properties at larger deformations, implying shear.

Several authors postulated that the cytoskeleton can be considered as a two-dimensional rubber-like network with the spectrin filaments forming entropy springs (Stokke et al. 1986). This would imply that the spectrin filaments behave as Rouse chains. But the q^4-dependence of the mean square amplitude $\langle u_q^2 \rangle$ (Zilker et al. 1987) is not consistent with Rouse behavior which would imply a q^2-dependence (De Gennes 1979). An interesting suggestion was made by Vertessy and Steck (c.f. Steck 1989) who conjectured that the entropic contribution to the membrane elasticity is a consequence of the hydrophobic effect associated with the spectrin folding during deformation.

The shear free (fluid-like) deformation regime of the cytoskeleton could also be due to the high density of defects of the quasi-triangular lattice. As shown by Nelson and Halperin (1979), the shear elasticity of such a network is very low if the conjugate pairs of $+60°$ and $-60°$ disclinations are dissociated. Above a critical strain the disclinations are expected to pair and the shear modulus increases.

Does the flickering serve a biological purpose? The membrane excitations are an intrinsic property of the membrane. Nevertheless, the undulations have two biologically interesting consequences. Firstly, the undulations lead to substantial dynamic repulsion forces (Helfrich 1978; Evans and Parsegian 1983) which could help to reduce the adsorption of the cells to the surface of the blood vessels. Secondly, the hydrodynamic flow in the cytoplasm associated with the undulations could facilitate the exchange of hemoglobin between the cytoplasm and the membrane surface.

Appendix

Evaluation of relative values of K_c and η from the integrated power spectrum $P(\omega)$. The integral of $P(\omega, q)$ (1)

with (2) and (3) is given by

$$P(\omega) = \frac{a}{\sqrt[6]{b}\,\omega^{5/3}}\left[\frac{1}{4\sqrt{3}}\ln\left(\frac{u^2+\sqrt{3}+1}{u^2-\sqrt{3}+1}\right)\right.$$
$$+\frac{1}{6}(\arctan(2u-\sqrt{3})+\arctan(2u+\sqrt{3})$$
$$\left.+2\arctan u)\right]_{u_{min}}^{u_{max}} \qquad (16)$$

where $u=\sqrt[6]{b/\omega^2}\,q$, $a=2Sk_BT/\eta$ and $b=(K_c/2\eta)^2$.

As noted above the frequency spectrum $F(\omega)$ is given by $F(\omega)=\sqrt{P(\omega)}$. In order to obtain η and K_c the Integral $P(\omega)$ has been numerically calculated for the integration limits $q_{min}=1\ \mu m^{-1}$ and $q_{max}=3\ \mu m^{-1}$ which are determined by the experimental conditions. The square root $\sqrt{P(\omega)}$ has been fitted to the experimental spectra $F(\omega)$ (normalized with respect to I_0, cf. experimental techniques) by variation of the residual adjustable parameters a and b. A least square fit procedure based on an algorithm of Marquardt (1963) has been used for this purpose. From the fitted parameters a and b relative values of the cytoplasmic viscosity η and the bending modulus K_c were obtained according to $\eta \propto 1/a$ and $K_c \propto \sqrt{b}/a$.

Acknowledgement. This manuscript was written during a sojourn of one of the authors (Erich Sackmann) as James visiting professor at the St. Francis University of Antigonish (Novo Scotia) and at UBC in Vancouver. He is most grateful to David Pink (Antigonish) for his help with the integration of the spherical harmonics and to Evan Evans for many enlightening discussions. Most helpful discussions with Narla Mohandas (University of San Francisco) and Conrad Pfafferott (Technische Universität München) concerning biomedical aspects of erythrocytes are gratefully acknowledged. Finally we gratefully recognize helpful suggestions concerning biochemical aspects by T. L. Steck. The work was supported by the Deutsche Forschungsgemeinschaft (Sa 246/20) and by the Fonds der Chemischen Industrie.

References

Backman L (1988) Functional or futile phosphorus? Nature 334:653–654

Bennett V (1989) The spectrin-actin junction of erythrocyte membrane skeletons. Biochim Biophys Acta 988:102–121

Bessis M, Mohandas N (1975) A diffractometric method for the measurement of cellular deformability. Blood Cells 1:307–313

Brochard F, Lennon JF (1975) Frequency spectrum of the flicker phenomenon in erythrocytes. J Phys 36:1035–1047

Bull BS, Weinstein RS, Korpman RA (1986) On the thickness of the red cell membrane skeleton: quantitative electron microscopy of maximally narrowed isthmus regions of intact cells. Blood Cells 12:25–42

Byers TJ, Branton D (1985) Visualization of the protein associations in the erythrocyte membrane skeleton. Proc Natl Acad Sci USA 82:6153–6157

Canham PB (1970) The minimum energy of bending as a possible explanation of the biconcave shape of the human red blood cell. J Theor Biol 26:61–81

Chasis JA, Mohandas N, Shohet SB (1985) Erythrocyte membrane rigidity induced by Glycophorin A ligand interaction – evidence for an ligand-induced association between Glycophorin A and skeletal proteins. J Clin Invest 75:1919–1926

Cohen CM, Foley SF (1980) Phorbol ester- and Ca^{++}-dependent phosphorylation of human red cell membrane skeletal proteins. J Biol Chem 261:7701–7709

Dall'Asta V, Gazzola GC, Longo N et al. (1986) Perturbation of Na^+- and K^+-gradients in human fibroblasts incubated in unsupplemented saline solutions. Biochim Biophys Acta 860:1–8

Deeley JOT, Coakley WT (1983) Interfacial instability and membrane internalization in human erythrocytes heated in the presence of serum albumin. Biochim Biophys Acta 727:293–302

De Gennes PG (1979) Scaling concepts in polymer physics. Cornell University Press, Ithaca

Deuling HJ, Helfrich W (1976) The curvature elasticity of fluid membranes: a catalogue of vesicles shapes. J Phys 37:1335–1345

Duwe H-P, Engelhardt H, Zilker A, Sackmann E (1987) Curvature elasticity of smectic A lipid bilayers and cell plasma membranes. Mol Cryst Liq Cryst 152:1–7

Duwe H-P, Eggle P, Sackmann E (1989) The cell-plasma membranes as a composite system of two-dimensional liquid crystal and macromolecular network and how to mimic its physical properties. Angew Makromol Chem 166:1–19

Engelhardt H, Sackmann E (1988) On the measurement of shear elastic moduli and viscosities of erythrocyte plasma membranes by transient deformation in high frequency electric fields. Biophys J 54:495–508

Evans EA (1973) Bending resistance and chemically induced bending moments in membrane bilayers. Biophys J 14:923–931

Evans E, Needham D (1986) Giant vesicle bilayers composed of mixtures of lipids, cholesterol and polypeptids. Faraday Discuss Chem Soc 81:267–280

Evans EA, Parsegian VA (1983) Energetics of membrane deformation and adhesion in cell and vesicle aggregation. Ann NY Acad Sci 416:13–26

Evans E, Skalak R (1980) Mechanics and thermodynamics of biomembranes. CRC Press, Boca Raton, Fla

Fricke K, Sackmann E (1984) Variation of frequency spectrum of the erythrocyte flickering caused by aging, osmolarity, temperature and pathological changes. Biochim Biophys Acta 803:145–152

Fricke K, Wirthensohn K, Laxhuber R, Sackmann E (1986) Flicker spectroscopy of erythrocytes. Eur Biophys J 14:67–81

Golan DE, Veach W (1980) Lateral mobility of band 3 in the human erythrocyte membrane studied by fluorescence photobleaching recovery. Evidence for control by cytoskeletal interactions. Proc Natl Acad Sci USA 77:2537–2541

Helfrich W (1973) Elastic properties of lipid bilayers: theory and possible experiments. Z Naturforsch 28c:693–703

Helfrich W (1978) Steric interaction of fluid membranes in multilayer systems. Z Naturforsch 33a:305–315

Hochmut RM, Worthy PR, Evans EA (1979) Red cell extensional recovery and the determination of membrane viscosity. Biophys J 26:101–114

Kapitza H-G, Sackmann E (1980) Local measurement of lateral motion in erythrocyte membranes by photobleaching technique. Biochim Biophys Acta 595:56–64

Khodadad JK, Weinstein RS (1983) The band 3-rich membrane of llama erythrocytes: studies on cell shape and the organization of membrane proteins. J Membr Biol 72:161–171

Leibler S, Singh RRP, Fisher ME (1987) Thermodynamic behavior of two-dimensional vesicles. Phys Rev Lett 59:1989–1992

Liu SC, Derick LH, Palek J (1987) Visualization of the hexagonal lattice in the erythrocyte membrane skeleton. J Cell Biol 104:527–536

Marquardt DW (1963) An algorithm for least square estimation of nonlinear parameters. J Soc Industr Appl Math 11:431–441

Milner ST, Safran SA (1987) Dynamical fluctuations of droplet microemulsions and vesicles. Phys Rev A 36:4371–4379

Nelson DR, Halperin BI (1979) Dislocation-mediated melting in two dimensions. Phys Rev B 19:2457–2483

Nelson GA, Andrews LA, Karnovsky MJ (1983) Control of erythrocyte shape by calmodulin. J Cell Biol 96:730–735

Ott P, Hope MJ, Verkleij AJ, Roelofsen B, Brodbeck U, van Deenen LLM (1981) Effect of dimyristoyl phosphatidylcholine on intact erythrocytes. Biochim Biophys Acta 641:79–87

Petersen NO, McConnaughey WB, Elson EL (1982) Dependence of locally measured cellular deformability on position on the cell, temperature and Cytochalasin B. Proc Natl Acad Sci USA 79: 5327–5331

Peterson MA (1985) Shape dynamics of nearly spherical membrane bounded fluid cells. Mol Cryst Liq Cryst 127:257–263

Petrov AG, Seleznev SA, Derzhanski A (1979) Principles and methods of liquid crystal physics applied to the structure and function of biological membranes. Acta Phys Pol A 55:385–405

Sackmann E, Duwe HP (1990) Bending elasticity and thermal excitations of lipid bilayer vesicles. Physica (in press)

Schneider MB, Jenkins JT, Webb WW (1984) Thermal fluctuations of large quasi-spherical bimolecular phospholipid vesicles. J Phys 45:1457–1472

Sheetz PM, Singer SJ (1974) Biological membranes as bilayer couples. A molecular mechanism of drug – erythrocyte interactions. Proc Natl Acad Sci USA 71:4457–4461

Shen BW, Josephs R, Steck TL (1984) Ultrastructure of unit fragments of the skeleton of the human erythrocyte membrane. J Cell Biol 99:810–821

Shohet SB, Nathan DG (1970) Incorporation of phosphatide precursors from serum into erythrocytes. Biochim Biophys Acta 202:202–205

Smith JE, Mohandas N, Shohet SB (1979) Variability in erythrocyte deformability among various mammals. Am J Physiol 236: H725–H730

Steck TL (1989) Red cell shape. In: Stein W, Bronner F (eds) cell shape: determinants, regulation and regulatory role. Academic Press, New York

Stokke BT, Mikkelsen A, Elgsaeter A (1986) Spectrin, human erythrocyte shapes and mechanochemical properties. Biophys J 49: 319–327

Svetina S, Zeks B (1989) Membrane bending energy and shape determination of phospholipid vesicles and red blood cells. Eur Biophys J 17:101–111

Takakuwa Y, Tchernia G, Rossi M, Benabadji M, Mohandas N (1986) Restoration of normal membrane stability to unstable protein 4.1 deficient erythrocyte membranes by incorporation of purified protein 4.1. J Clin Invest 78:80–85

Waugh RE (1987) Effects of inherited membrane abnormalities on the viscoelastic properties of erythrocyte membrane. Biophys J 51:363–369

Yoshino H, Minari O (1987) Heat-induced dissociation of human erythrocyte spectrin dimer into monomers. Biochim Biophys Acta 905:100–108

Zilker A, Engelhardt H, Sackmann E (1987) Dynamic reflection interference contrast (RIC-) microscopy: a new method to study surface excitations of cells and to measure membrane bending elastic moduli. J Phys 48:2139–2151